ORIGINAL RESEARCH

Examining the Synergism of Cerium Oxide Nanoparticle – Andrographolide Conjugate and Studying its Potential Role Towards Antioxidative Therapeutics

Article history:
Received: 30-05-2024
Revised: 23-09-2024
Accepted: 28-11-2024
Published: 14-12-2024

Sneha Kumari[a], Shivam Pandey[b], Leela Manohar Aeshala[c], Anuj Kumar[d], Sushant Singh[e]

Abstract: Increased oxidative stress in metabolic disorders has revealed promising alternatives for antioxidative therapeutics. Herein, we present synthesis and evaluations of Cerium oxide nanoparticles (CNPs) conjugated with Andrographolide (Ad-CNP). Characterization revealed a uniform particle size of 106 nm for bare CNP and 120 nm for Ad-CNP conjugates. UV-visible spectroscopy showed an absorbance peak at 230nm, indicating a high Ce^{3+}/Ce^{4+} oxidation state. X-ray diffraction confirmed a pure cubic fluorite structure with a polycrystalline nature with peaks at 111, 200, 220, and 311. In terms of reactive oxygen species scavenging, bare CNPs demonstrated Catalase mimetic activity of 41.5%, whereas the Ad-CNP conjugates showed 47% scavenging activity. The Superoxide Dismutase mimetic activity was significantly increased due to synergy up to 77% of Ad-CNP whereas bare CNPs showed 57% activity. The CNPs exhibited notable antibacterial efficacy, diminishing microbial proliferation by 69% for bare CNPs and 82% for Ad-CNP. Biocompatibility testing with human skin keratinocytes validated the safety of the nanoparticles, and anti-inflammatory assays indicated decreased expression of pro-inflammatory cytokines IL-6 and TNF-α. The synergistic combination of CNPs with Andrographolide demonstrated significant potential as a potent antioxidant, antibacterial, and anti-inflammatory agent, making it a prospective candidate for antioxidative therapeutic research aimed at diminishing oxidative stress.

Keywords: Cerium oxide Nanoparticles; Andrographolide; Catalase; Superoxide Dismutase; Biocompatibility; Anti-inflammatory, Antimicrobial.

[a] Amity Institute of Biotechnology, Amity University Chhattisgarh, Raipur - 493225, Chhattisgarh, India.

[b] Amity Institute of Biotechnology, Amity University Chhattisgarh, Raipur - 493225, Chhattisgarh, India.

[c] Department of Chemical Engineering, National Institute of Technology Warangal, Telangana-506004, India.

[d] School of Materials Science and Technology, Indian Institute of Technology (BHU), Varanasi 221005, India.

[e] Department of Life Sciences, Sharda School of Basic Sciences and Research, Sharda University, Greater Noida-201310, Uttar Pradesh, India.
Corresponding author: drssingh1983@gmail.com

INTRODUCTION

In the past decade, nanotechnology has advanced significantly, leading to major changes in multiple industries, such as electronics, medicine, energy, and the environment. Among the various types of nanomaterials, cerium oxide nanoparticles (CNP) have attracted significant attention due to their unique physical and chemical properties, including optical, biological, electrical, and catalytic capabilities. CNPs special redox nature makes them highly useful in several fields, including fuel cells, catalysis, solar cells, sensors, and drug delivery devices (Ray *et al.*, 2012; Montini *et al.*, 2016). However, the traditional method of producing CNPs often involves hazardous chemicals

and energy-intensive processes that negatively impact the environment. As a result, scientists are increasingly turning to environmentally safe and sustainable methods to develope nanoparticles. One promising method is the use of plants for creating nanomaterials. This approach offers many benefits, such as cost-effectiveness, biocompatibility, and low use of hazardous substances (Singh *et al.,* 2020; Singh *et al.,* 2021: Dowding *et al.,* 2014. *Andrographis paniculata*, commonly known as the "king of bitters," is a herbaceous plant belonging to the Acanthaceae family. It is found in tropical and subtropical regions of Asia, including Southeast Asia and India. This plant is known as "Kalmegh" in India, "Chuan-Xin-Lian" in China, "Fah Tha Lai" in Thailand, "Hempedu bumi" in Malaysia, "Senshinren" in Japan, and "Green chiretta" in Scandinavian countries. The extracts of *A. paniculata* and its primary constituent, Andrographolide, have various pharmacological properties, including immunostimulatory, antimicrobial, anti-diabetic, and anti-cancerous (Zhao *et al.,* 2020; Tian *et al.,* 2020).

Plant-based substances and their derivatives are primary sources of bioactive molecules, with diterpenoids constituting a substantial library of potential compounds for novel drug discovery (Amaning *et al.,* 2022). The naturally occurring diterpenoid andrographolide has garnered significant attention and has been utilized in clinical examinations for an extended period. Since the identification of andrographolide more than a century ago, significant endeavors have been undertaken to develop novel powerful analogs with various applications (Thammawithan *et al.,* 2022). Research has shown that using plant extracts, like *Andrographis paniculata,* is important for developing new antioxidant compounds. Andrographolide, that has strong anti-mycobacterial properties and helps prevent atherosclerosis by reducing the production of inflammatory mediators such as IL-6 and MCP-1, as well as the production of ROS (Hossain *et al.,* 2021). Due to its ROS scavenging property, it is reported to be an eminent anti-microbial compound when combined with preliminary antibiotics, on the other hand, conjugation of Andrographolide with other nanoparticles shows enhanced biomedical activities such as Andrographolide coated with silver nanoparticles and gold nanoparticles show antifilarial property (Yadav *et al.,* 2020), decreases antibiotics resistance (Thammawithan *et al.,* 2022; Do Dat *et al.,* 2023). Due to the diversity of these biological actions, researchers suggest exploring more leads through the structural modification of Andrographolide. In the last few decades, there has been a surge of Andrographolide derivatives that have been extensively studied for their pharmacological properties. Cerium oxide nanoparticles (CNPs) on the other hand are a type of nanomaterial that possess antioxidant-like activity. These nanoparticles have been shown to have various therapeutic applications, such as anti-inflammatory properties, defense against cell death and radiation-induced toxicity, and promise for cancer therapy, wound healing and tissue repair (Mustafa *et al.,* 2021). CNPs are highly versatile and have been extensively studied for a wide range of biological purposes, from brain health protection to cancer research, in both laboratory and real-world settings. The exceptional antioxidative properties of CNPs are attributed to the presence of cerium oxide ions in multiple oxidation states (Ivanov *et al.,* 2009). The nanoparticles typically exist in two main oxidation states, cerium (III) oxide and cerium (IV) oxide, which are similar to their bulk counterparts. However, the unique catalytic properties of CNPs are due to their large surface area and the presence of oxygen. The formation and elimination of oxygen vacancies inside the cerium lattice create catalytic hotspots that enhance the nanoparticles' ability to scavenge reactive oxygen species (ROS). Nanoceria can counteract ROS through various mechanisms that depend on their oxidation state. These mechanisms include the reactions of Catalase and Superoxide Dismutase (SOD), which are commonly seen in biological systems. The effectiveness of nanoceria as an antioxidant is due to its ability to transition between two distinct cerium oxidation states, cerium (III) oxide and cerium (IV) oxide. This allows for the continuous scavenging of ROS. The ratio of oxidation states of cerium oxide, Ce^{3+}/Ce^{4+}, significantly affects the enzymatic activity of CNPs (Campbell & Peden, 2005). For instance, CNPs with a high ratio of Ce^{3+} to Ce^{4+} have the potential to mimic superoxide dismutase (SOD), while CNPs with a lower ratio exhibit activity similar to Catalase. The synthesis process plays a crucial role in protecting against oxidative stress and maintaining a balance between cellular oxidants and reducing agents, thanks to the important antioxidative enzymes SOD and Catalase. Henceforth, this work aims to provide a scholarly contribution to the current advancements in Andrographolide research by presenting comprehensive insights into the enhanced pharmacological properties of Andrographolide and Cerium oxide Nanoparticle conjugate *(Ad-CNP)* due to their combined synergistic effects.

METHODS AND MATERIALS

Materials

Cerium Nitrate Hexahydrate (Catalogue. No – GRM1441) from Hi-Media, Andrographolide (Sigma), 30% H_2O_2 (Cat. No- PCT1511), Ascorbic acid (Cat. No – 01550, by Loba Chemie), Nitrobule Tetrazolium (Cat. No. RM578 by Hi-Media), Methionine (Cat. No. PCT0315, by Hi-Media), LB Broth (Cat. No. G008, Make- Hi-Media), α-amylase (Cat. No. GRM638, Make- Hi-Media), starch (Cat. No.GRM424, Make- Hi-Media), Di-nitrosalicylic acid (Cat. No.128848, Make-Sigmaldrich), and Acarbose (Cat. No.A8980, Make-Sigmaaldrich).

Synthesis of cerium oxide nanoparticles and *Ad-CNP*

Cerium Nitrate Hexahydrate was used as a precursor source for the synthesis of cerium oxide nanoparticles. A stoichiometric amount of Cerium Nitrate Hexahydrate was added and dissolved in 35 ml of distilled water, the solution was properly stirred until it turned crystal clear. Once the clear solution was obtained, an aqueous solution of 30% Ammonium Hydroxide (oxidizer and mineralizer) was added to the solution and stirred to obtain a clear solution of the nanoparticle. The obtained mixture was then further centrifuged at 4,000 rpm for refinement and the synthesis was confirmed by the last step through calcination at 600°C for 40 minutes via a dual wet chemical approach whereas the conjugate nanomaterial of Andrographolide and Cerium oxide Nanoparticles *(Ad-CNP)* were synthesized via mixing a stoichiometric amount of Cerium nitrate hexahydrate in 35 ml of distilled water, the solution was properly stirred until it turned crystal clear. Once the clear solution was obtained aqueous solution of plant extract (1mg/ml) was added to the solution and stirred to obtain a homogenized mixture of inter-fused nanomaterials. The obtained mixture was then further centrifuged at 4,000 rpm for refinement and the conjugation was confirmed by the last step of synthesis through calcination at 600°C for 40 minutes (Yeh *et al.,* 2018).

UV-visible, DLS, XRD and SEM Characterization

UV-visible spectroscopy (UV-Vis) and dynamic light scattering (DLS) were utilized to analyze the synthesized materials. The Novostrix Nanodrop UV visible device was used to obtain the UV-Vis spectra. Confirmatory peaks were found in the range of 220-720 nm, indicating the surface oxidation state of Ce^{4+}. The size distribution of the synthesized samples was determined to be in the range of 50 to 250 nm by examining the hydrodynamic radius using a Litesizer 500 device for DLS analysis. Before analysis, the samples were subjected to ultrasonication for 15 minutes to ensure complete dispersion of particles in the solution. The XRD method was used to investigate the crystalline nature of the nanomaterial sample, and the resulting planes were used to determine its crystalline arrangement (Keyvan Rad *et al.,* 2018; Xu *et al.,* 2013).

Analysis of antioxidative and antimicrobial Activity

The synthesized CNP materials were subjected to antioxidant research to assess their catalase and superoxide dismutase mimetic activity. A reaction mixture comprising 30 µl of CNP, 50 mM, PBS Buffer and 20 mM H_2O_2 was made to measure the catalase activity. The spectrophotometer was used to monitor the consumption of H_2O_2 at a wavelength of 240 nm, with observations performed at 15-minute intervals. The researchers were able to assess the extent of H_2O_2 breakdown by observing the decrease in absorbance over a while (Celardo *et al.,* 2011; Karakoti *et al.,* 2010). The Nitro Blue Tetrazolium (NBT) approach was used to conduct the superoxide dismutase (SOD) test. The experimental procedure consisted of three tubes, namely a blank (B), a test (T), and a control (C). The absence of CNP nanoparticle samples was seen in the Blank tube, which included Methionine, riboflavin, and phosphate buffer. The Test tube, denoted as T, consisted of identical components to the Blank tube, with the inclusion of a CNP nanoparticle solution that has undergone independent testing to assess its potential as a surface oxidase (SOD) mimic (Heckert *et al.,* 2008). The concentration range at which nanoparticles impede bacterial growth was determined by diluting a starting solution of nanoparticles into aseptic growth media. An E. coli culture was then cultivated and manipulated to achieve the desired cell density. The nanoparticle solutions were diluted and then introduced into test tubes containing standardized E. coli cultures. The tubes and culture plates were then subjected to an incubation period of 14 hours at a temperature threshold of

37°C. The turbidity of the broth solution was visually assessed for the presence of observable bacterial growth after the incubation period. The quantitative assessment included measuring the optical density (OD) at a wavelength of 600 nm (Griendling *et al.*, 2016).

Cellular Biocompatibility and Anti-inflammatory Assessment

The HACAT cell line was used to conduct the MTT-based Cytotoxicity assay of the CNP sample. The experiment began by seeding a 96-well plate with 5,000 cells ($5x10^3$) in each well. The plates were then grown at a temperature of 37°C in a 5% CO_2 incubator for 48 hours. To ensure consistency, the experiment was repeated five times. After 48 hours, the CNP sample was added to each well at a concentration of 5mg/ml, followed by the addition of 5mg/ml of MTT reagent. The plate was then reintroduced into the incubator for another 4 hours. After this, the MTT solution was removed, and 100µl of DMSO was added to each well to carefully dissolve the Formazan crystals. The percentage of cell viability was determined by measuring the absorbance at a wavelength of 570 nm using the following formula: [OD (Treated) / OD (Control)] x 100.

To maintain and cultivate human monocyte-derived cells, a solution containing 100 U/ml of penicillin-streptomycin (antibiotics) and 10% fetal bovine serum (FBS) in RPMI medium was used. The cells were kept in an incubator at a temperature of 37°C with a CO_2 concentration of 5%. The cells were then exposed to lipo-polysaccharides (LPS) at a concentration of 100 ng/ml for 24 hours to induce the production of inflammatory cytokines. After that, the effect of pharmaceuticals on cytokine production was assessed by using a medium control and drug concentrations of 250g/ml (CNP, IC50 conc.) for 24 hours. The cells were then subjected to RNA extraction using Sigma Aldrich's Trizol reagent, following the manufacturer's instructions. The resulting RNA was converted to cDNA using the Aurea cDNA synthesis kit, following the manufacturer's instructions. Finally, gene expression analysis was conducted using real-time PCR for two inflammatory cytokines: TNF-alpha and IL-6. The forward primer for TNF alpha is CCTCTCTCTAATCAGCCCTCTG, and the reverse primer for TNF alpha is GAGGACCTGGGAGTAGATGAG. Likewise, the forward primer for IL-6 is ACTCACCTCTTCAGAACGAATTG, and the reverse primer for IL-6 is CCATCTTTGGAAGGTTCAGGTTG. B-actin was used as a housekeeping gene. The relative gene expression data obtained from qPCR were analyzed using the ddCt technique.

RESULTS

Synthesis of Cerium Oxide Nanoparticles and *Ad-CNP*

Numerous approaches have been reported for the synthesis of cerium oxide nanoparticles. Herein we report a dual wet chemical approach including oxidation and further combustion process leading to the synthesis of nanoparticles. Cerium Oxide Nanoparticles were synthesized by implementing two methods of wet chemistry – oxidation method using ammonium hydroxide as oxidizer as well as mineralizer to initiate the nucleation process. The second applied technique was the combustion method in which obtained nanoparticles were calcinated at 600°C for further annealing of nanoparticles. On the other hand, Andrographolide and Cerium oxide nanoparticle *(Ad-CNP)* conjugate were successfully synthesized using the protocols of green chemistry using Andrographolide as the oxidizer as well as stabilizing agent in the synthesis of conjugated nanomaterial. *Ad-CNP* conjugate nanomaterial after calcination was subjected to characterization for further studies.

Characterization of Cerium oxide Nanoparticles

The preliminary confirmation of nanoparticle fabrication was performed utilizing UV-visible spectroscopy. The absorbance range obtained at 230 nm indicated a larger ratio of Ce^{3+} to Ce^{4+} oxidation state, as shown in (Fig. 1a). Dynamic Light Scattering (DLS) Analysis was used to determine the size of the nanoparticles, revealing a hydrodynamic radius of 110 nm- Bare CNP and 120nm of *Ad-CNP* (Fig. 1b). The SEM was used to thoroughly analyze the surface of the produced Cerium Oxide Nanoparticles (Fig. 2A). X-ray Diffraction examination verified the existence of crystals in both the Cerium Oxide Nanoparticles, as shown by the confirming peak seen at planes of crystals 111, 200, 211, and 311 (Fig. 2b). FTIR analysis was conducted to examine the presence of groups with functional properties on Cerium Oxide Nanoparticles. The study identified specific peaks associated with Cerium Oxide Nanoparticles (Fig. 3).

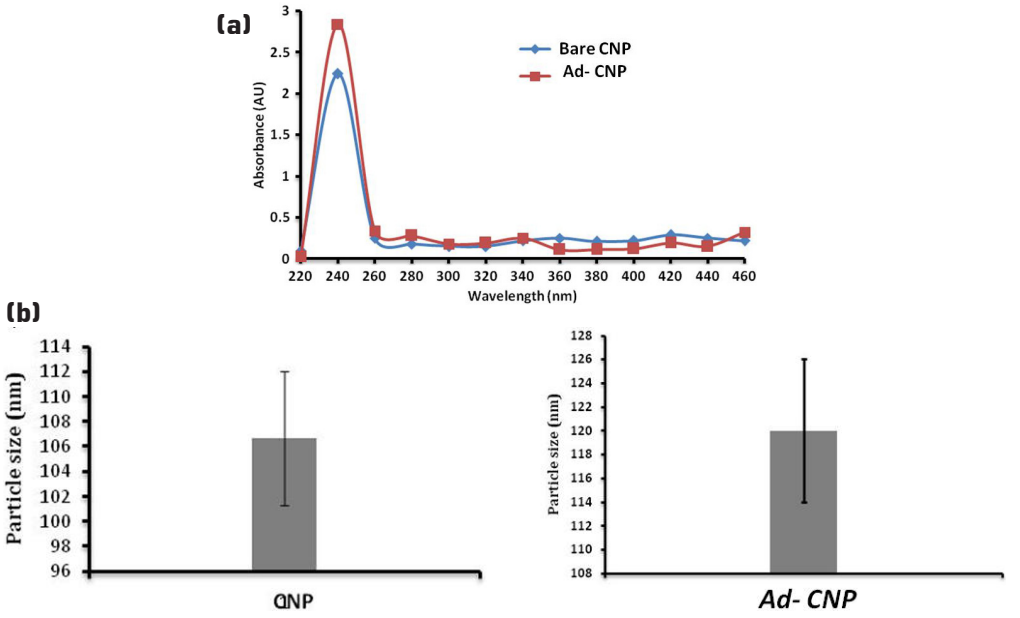

Figure 1. Represents the UV Visible and Dynamic Light Scattering (DLS) characterization of the synthesized CNP and *Ad-CNP*. (a) indicated the peak obtained at 230nm shows the presence of Ce^{+3} oxidation state of synthesized nanomaterials. (b) indicates the DLS characterization for the size analysis of synthesized nanoparticles. The hydrodynamic radius of synthesized bare CNP and *Ad-CNP* was found to be in the range of 106.66nm and 120nm respectively.

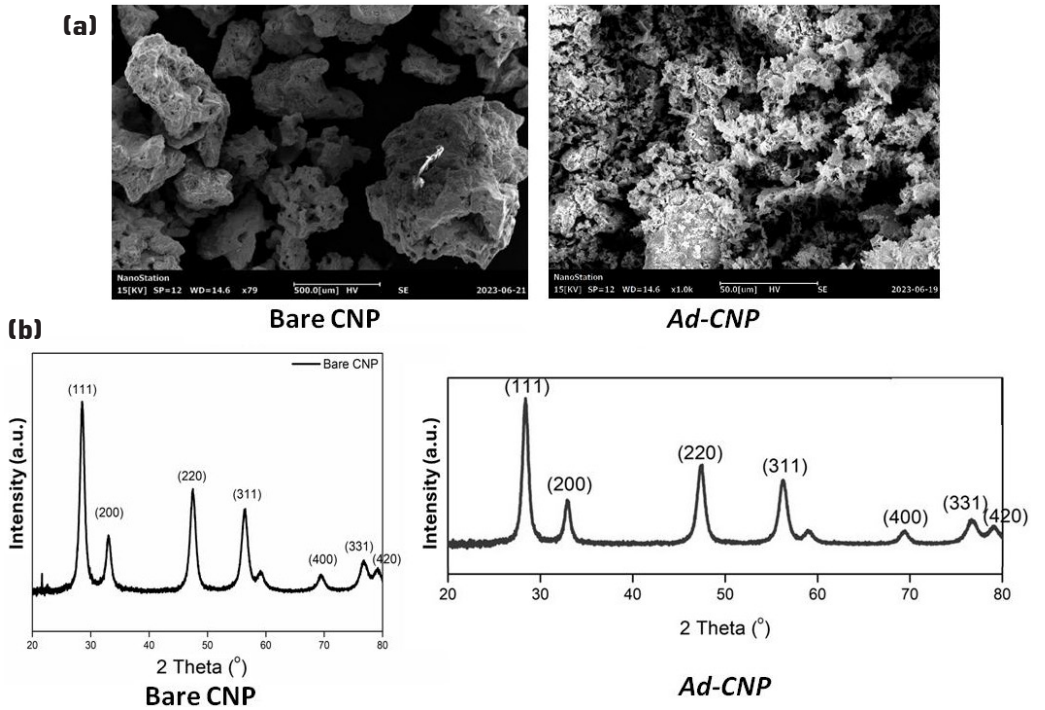

Figure 2. Represent the Scanning Electron Microscope (SEM)and X-ray Diffraction analysis of the synthesized cerium oxide nanomaterials. (a) represents the SEM image of the ultrafine powder of synthesized bare CNP and *Ad-CNP*. (b) represents the XRD graph obtained for the bare CNP and *Ad-CNP*. The graph indicates that relevant signatory planes of the cerium oxide nanoparticle which are 111,200, 220, and 311 planes and indicative of the crystalline nature of the cubic fluorite structure synthesized.

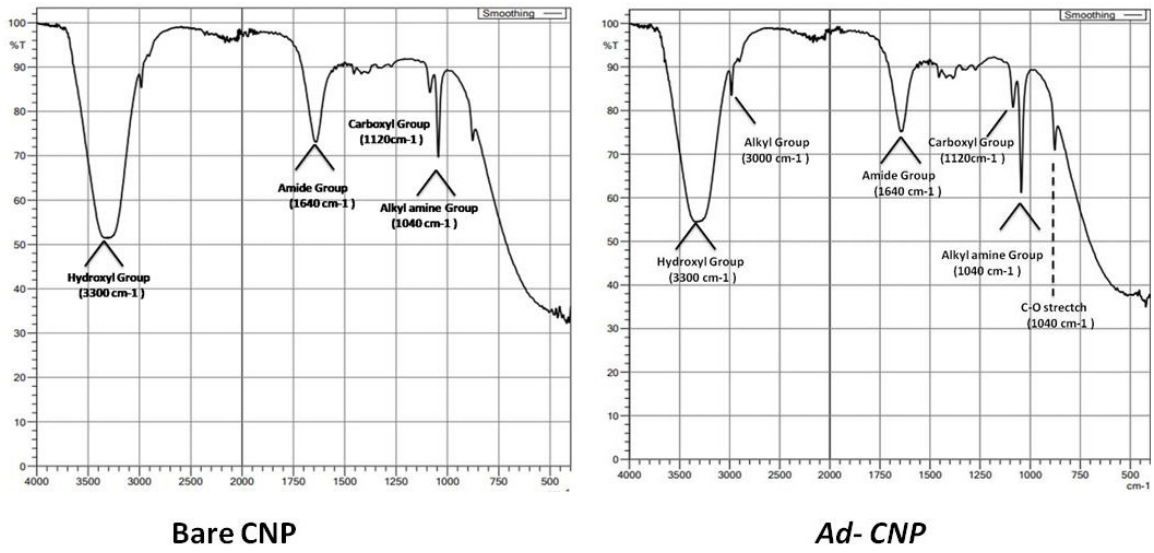

Figure 3. Represents the FTIR spectra of the synthesized CNP nanomaterials. Specific peaks were obtained in all the different formulations of bare CNP, Amine C-H stretching (1409), Aromatic C-C stretch (1543) and bare CNP such as Hydroxyl group at (3300), Amide group (1640) and O-H bending at 1204 cm^{-1} were visible.

Antioxidative-Reactive Oxygen Species (ROS) Scavenging analysis

The antioxidative effectiveness of the Cerium Oxide Nanoparticles was measured using biochemical tests for both Catalase and SOD mimic activities. Biochemical analysis was used to quantify the H_2O_2 degradation parameters to determine the Catalase mimetic activity. The results showed that CNP and *Ad-CNP* displayed varying levels of scavenging activity (as shown in Fig 4). The CNP demonstrated a moderate level of H_2O_2 scavenging activity of 41.9% whereas due to synergistic effects, the Catalase mimetic activity of *Ad-CNP* was observed to be 47.03%. Additionally, the concentration of CNP sample assessed was directly proportional to the H_2O_2 scavenging activity. The NBT reduction test was used to investigate the SOD mimic activity of the CNP, riboflavin-methionine was used to produce superoxide radicals and examine the SOD mimic activity of the CNP. The results showed that the SOD mimetic activity of CNP was 57.8% whereas due to synergistic effects, the SOD activity of *Ad-CNP* was assessed to be 77%.

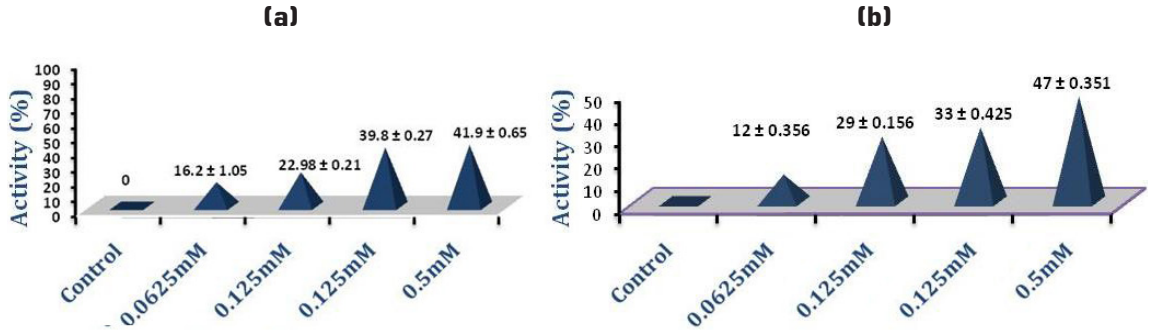

Figure 4 (a & b). Represents the Catalase mimetic activity of synthesized bare CNP and *Ad-CNP* respectively. Catalase mimetic assay demonstrated the H_2O_2 scavenging activity of CNP at different concentrations. All the experiments were performed in triplicate and the data are presented in the form of Mean ± S.D

 https://doi.org/10.37819/nanofab.9.2031

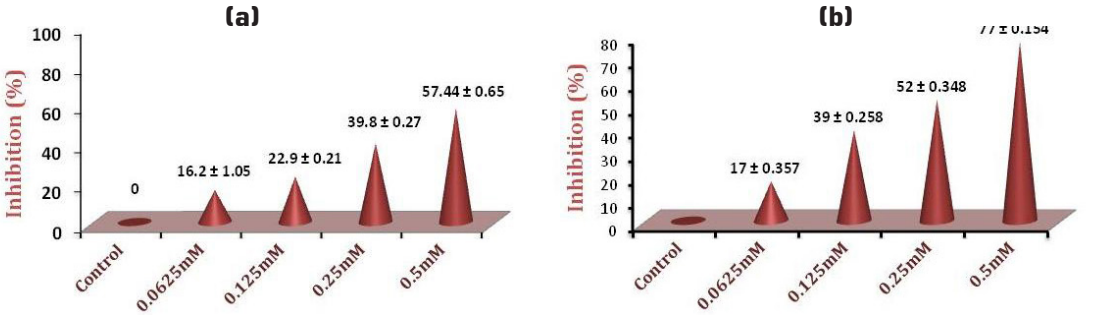

Figure 5 (a & b). Represents the superoxide dismutase mimetic activity of synthesized bare CNP and *Ad-CNP* respectively Superoxide Dismutase mimetic assay demonstrated the superoxide ions scavenging activity of CNP nanomaterials. All the experiments were performed in triplicates and the data are presented in the form of Mean ± S.D

Antimicrobial Potential of Cerium Oxide Nanoparticles

To assess the antimicrobial potential of Cerium oxide Nanoparticles Minimum Inhibitory Concentration (MIC) assay was performed using 10^6 folds of *E. coli.* It was observed that the antimicrobial activity of obtained Bare CNP was up to 69% at the concentration of 0.5 mM whereas the antimicrobial activity of *Ad-CNP* was 82%. Through the assessment of nanoparticles at different ranges of concentrations, it was observed that the activity was directly proportional to the increase in the concentration of the sample (Cerium oxide Nanoparticles) as depicted in Fig 6a & b. A second set of experiments was performed to study the antimicrobial potential of Cerium oxide Nanoparticles in which the glass slides coated with Bacterial inoculums were treated with Cerium oxide Nanoparticles solution and it was clearly observed that the side treated with Cerium oxide Nanoparticles showed clear zones in comparison to the untreated side as depicted in Fig 6c & d.

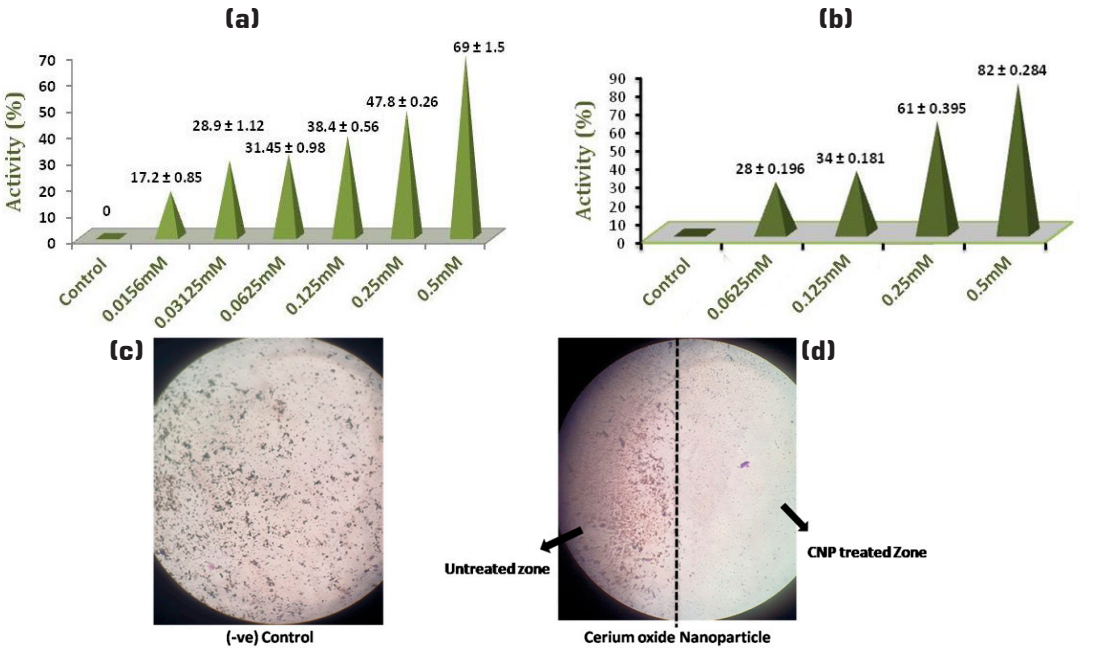

Figure 6. Represents the antimicrobial efficiency of CNP against 10^6 folds E.coli Culture. (a & b) Shows the absorption and percentage inhibition of CNP at different concentrations of 0.5 mM, 0.25 mM, 0.125mM, and 0.0625mM of Bare CNP and *Ad-CNP* respectively. All the experiments were performed in triplicates and the data are presented in the form of Mean ± S.D. (c & d) Showing the antimicrobial efficiency of CNP via surface coating on the slide about negative control.

Cellular Biocompatibility assessment

The biocompatibility of CNP was assessed using the HaCat cell line, a human skin keratinocyte cell line. Different concentrations of CNP and *Ad-CNP* solutions, including 0.5µM, 0.25µM, 0.125µM and 0.0625µM, were used in the experiment. After the treatment, an MTT study was conducted to evaluate the impact on biocompatibility, which revealed that synthesized CNP exhibited cell-based biocompatibility. The viability levels of HaCat cells treated with CNP were approximately close to 71% of Bare CNP and the conjugated nanoparticle *Ad-CNP* had a remarkable viability of 89% at a concentration of 0.5µM, indicating its nontoxic nature as shown in Fig. 7a & b. The results of the biocompatibility investigation conducted for different concentrations were evaluated. This suggests that CNP and its conjugate *Ad-CNP* may efficiently remove ROS from the biological system when it interacts with them.

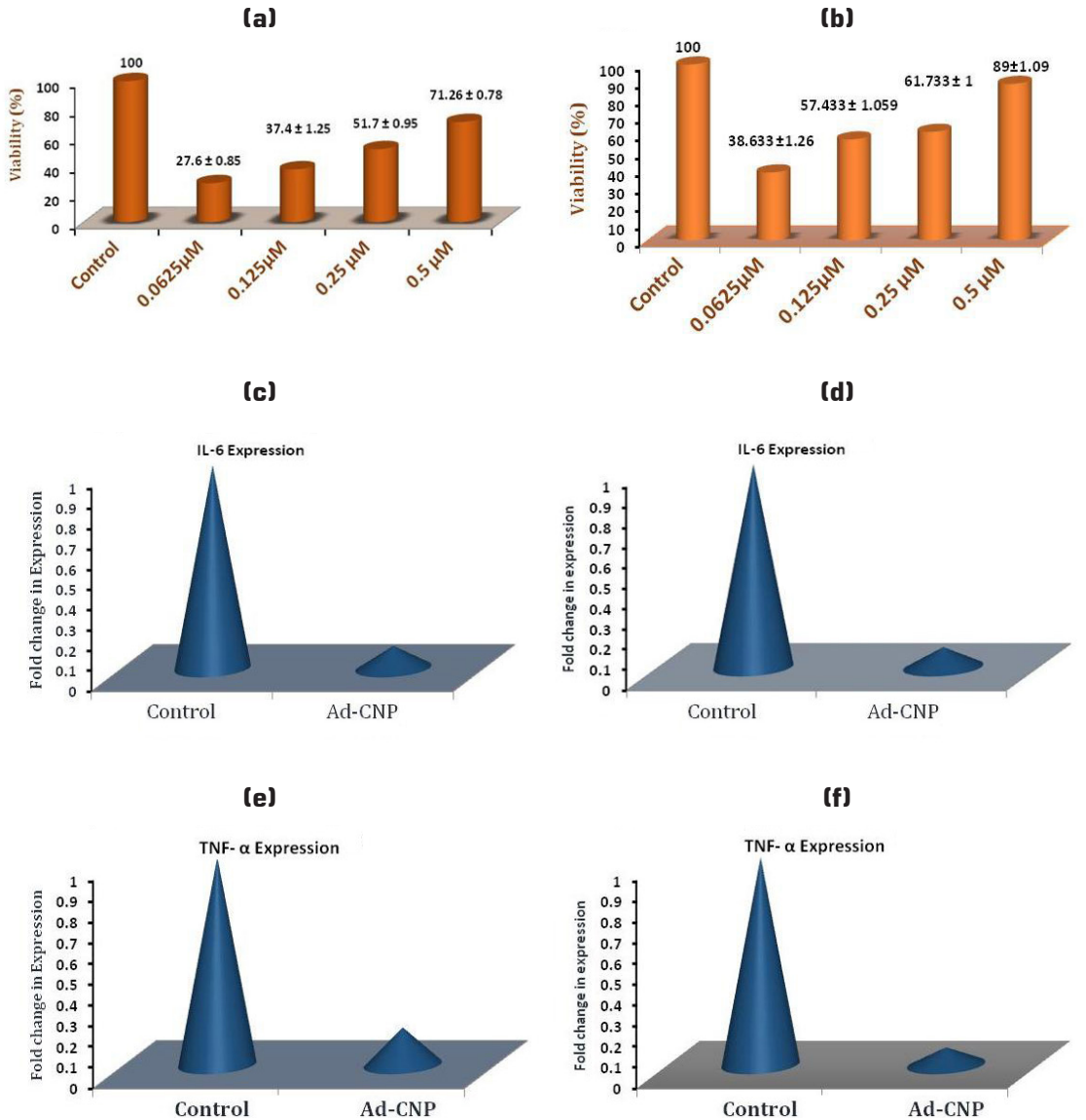

Figure 7. Represents the Biocompatibility and Anti-inflammatory efficiency of CNP. (a & b) shows the Biocompatibility percentage of bare CNP and *Ad-CNP* at different concentrations. (c, d, e, & f) shows folds of changes observed in IL-6 expression and TNF-α expression levels respectively of Bare CNP and *Ad-CNP* in comparison to the control treatment. All the experiments were performed in triplicates and the data are presented in the form of Mean± S.D.

 https://doi.org/10.37819/nanofab.9.2031

Anti-inflammatory assessment

For the Anti-inflammatory assay, U937 cells (Human Monocytes derived) were used for studies and maintained in 10% FBS containing RPMI media with 100U/ml penicillin-streptomycin (antibiotics). The activity was calculated based on the folds of reduction in expression of TNF-α and IL-6. It was observed that the synthesized CNP exhibited anti-inflammatory properties by reducing the IL-6 (Interlukein-6) and TNF-α expression to 89% and 82% respectively as shown in Figs 7 (c, d, e & f) due to synergistic effect the anti-inflammatory effect was assessed to be 90.1% and 91.6% respectively. It can be concluded from the obtained results of suppression folds that the synthesized Cerium oxide nanoparticles were effective in reducing the levels of cytokines involved in inflammation leading to reduced inflammatory responses.

DISCUSSION

Nanotechnology has expanded significantly, and it is being used in multiple industries due to the unique physical and chemical properties of nanoparticles. NPs possess enhanced functionalities in catalysis, mechanics, chemistry, and biology (Karakoti *et al.*, 2010 (b)). They have a high level of reactivity and mobility, and they exhibit exceptional dissolving capabilities and strength due to their elevated surface-to-volume ratio. NPs are generated using several methodologies and can also be found in nature on Earth, originating from sources such as soil, water, volcanic dust, and minerals (Yokel *et al.*, 2014; Dziubla *et al.*, 2008). They are used in various industries, including food & drinks, agriculture, and medicines. Scientists worldwide are showing significant interest in using nanoparticles in biocompatible materials for the development of hybridized scaffolds. Among all the nanoparticles, Cerium has been produced using various methods, the method of synthesis defines its characteristic features and efficacy in other fields (Chen *et al.*, 2018; Shuvaev *et al.*, 2013). We used Ammonium Hydroxide as an oxidizing as well as mineralizing agent and Cerium nitrate hexahydrate as the precursor to synthesize cerium oxide nanoparticles. The obtained transparent nanoparticle solution was then calcinated at a high temperature of 600°C for nanoparticle annealing. The self-propagating high-temperature synthesis technique is a rapid and effective way of producing a diverse range of nanoparticles. In contrast to the oxidation technique, which requires an oxidizing agent, this approach is simpler and does not involve the use of any additional chemicals (Xia *et al.*, 2008; Miri & Sarani, 2018). The method can be classified into three types, depending on the physical properties of the initial reaction medium: condensed phase combustion or conventional SHS (involving a solid initial reaction medium), solution-combustion synthesis (involving reactants in an aqueous state), and gas phase combustion (involving the synthesis of nanoparticles in a flame). To synthesize Cerium Oxide Nanoparticles, we combined oxidation-based synthesis and combustion techniques (Darroudi *et al.*, 2014; Kartha *et al.*, 2022; Poole *et al.*, 2015). This approach resulted in the successful synthesis of Cerium Oxide Nanoparticles, with a hydrodynamic radius of around 110 nm, which defines its distinctive behavior in contrary to the conjugated Cerium oxide nanoparticle *Ad-CNP* was synthesized *via* the protocol of green chemistry where no extra chemicals were added as oxidizer or mineralizer but the Andrographolide was mixed into 0.1 M solution of Cerium nitrate hexahydrate and conjugation was confirmed upon annealing through calcination at 600°C for 40 minutes fine yellow powder of *Ad-CNP* was obtained with hydrodynamic radius of 120nm confirmed through DLS and its further properties were assessed to evaluate the impact of conjugation.

The developed cerium oxide nanoparticles exhibit intriguing biological applications. The synthesis confirmation was accomplished by various physicochemical characterization methods. The primary confirmation was achieved using UV-visible spectroscopy (Fig. 1a), revealing a greater Ce^{+3}/Ce^{+4} oxidation state, correlated with enhanced superoxide dismutase mimetic activity, in contrast to catalase mimetic activity, aligning with previous studies (Shuvaev *et al.*, 2007; Fard *et al.*, 2015). The surface morphology was analyzed using scanning electron microscopy (SEM) to elucidate its morphological properties (Fig. 2a). XRD confirmed the existence of a crystalline structure in the nanomaterials. The crystallinity of the produced nanomaterial was compared to previously published studies, revealing that the Cerium Oxide Nanoparticles exhibit a crystallinity of 98% for Bare CNP and 82% for *Ad-CNP* (Fig. 2b). FTIR was performed to verify the presence of active chemicals and to identify the individual compounds in the produced

nanomaterials (Fig. 3) (Dowding *et al.*, 2012). Fig.4 indicates that the catalase mimetic activities of cerium oxide nanoparticles were 41.9% for bare CNP and 47.03% for *Ad-CNP*. Fig. 5 illustrates that the SOD mimetic activity was recorded at 57% for Bare CNP and 77% for *Ad-CNP* (Sisubalan *et al.*, 2018; Nelson *et al.*, 2016). The antibacterial efficacy of the produced Cerium Oxide Nanoparticle was recorded at 69% for Bare CNP and 82% for *Ad-CNP*, as illustrated in Fig. 6. Cerium oxide nanoparticles with an optimal Ce^{+3}/Ce^{+4} ratio diminish free radical production and modify the structure of bacterial cell wall membranes, hence exhibiting antibacterial characteristics (Dhall & Self, 2018). Fig. 7 displays the outcomes of the in vitro assessment of cerium oxide nanoparticles at varying concentrations for biocompatibility and anti-inflammatory evaluation. An MTT assay was performed post-treatment to assess biocompatibility effects. The findings demonstrated that both the Bare CNP and the Adsorbed CNP exhibited cellular biocompatibility. HaCat cells subjected to Cerium Oxide Nanoparticles at a concentration of 0.5µM exhibited a cellular vitality of around 71% and 89%, indicating minimal cellular toxicity according to the existing literature (Xu & Qu, 2014). The biocompatibility investigation was conducted at various dosage levels, utilizing U937 cells derived from human monocytes for the anti-inflammatory assay. The activity level was evaluated by quantifying the decrease in the expression of TNF-α and IL-6. Cerium Oxide Nanoparticles demonstrated anti-inflammatory properties by drastically decreasing the expression of IL-6 (Interleukin-6) and TNF-α by 89% and 81% for Bare CNP, and by 90.1% and 91.6% for *Ad-CNP* (Davies & Wright, 1997; Chen *et al.*, 2021; Tian *et al.*, 2020). Reduced levels of these cytokines indicate effective modulation of inflammatory mediators. We have successfully synthesized an efficient nanoparticle exhibiting enhanced biomedical properties, including superoxide dismutase activity, moderate catalase mimetic activity, anti-inflammatory effects, and antibacterial activity, by employing two methods within a single synthesis channel for bare CNP and green chemistry protocols for the synthesis of *Ad-CNP*. The nanoparticle size was approximately 100 nm, which influences its unique behavior. The comparison analysis demonstrates a beneficial synergistic effect of conjugation, highlighting the bio-sustainable synthesis strategy in relation to biomedical efficacy.

CONCLUSION

In this study, we provide the first evidence of the sustainable production of cerium oxide nanoparticles using Andrographolide. The procedure facilitates the advancement of redox-active cerium oxide nanomaterials that exhibit exceptional features in scavenging reactive oxygen and reducing oxidative stress. This collaboration also results in potential use in the field of antimicrobials for the use of synthesized nanomaterials, as shown by the collected data. To our surprise, the results have shown that the synthesized *Ad-CNP* conjugates have the potential to operate as anti-oxidative, anti-microbial, and anti-inflammatory agents by reducing the production of TNF-alpha and IL-6 factors. It is expected that these discoveries will greatly contribute to the advancement of pharmaceutical research, particularly in terms of enhancing the creation of medications from the perspective of biology. ♦

REFERENCES

Amaning Danquah, C., Ofori, M., Gibbons, S., Bhakta, S., & Doe, P. (2022). Antibacterial and Antifungal Activities of Andrographolide in Combination with Antimicrobial Drugs. Research Journal of Pharmacognosy, 9(4), 21-27.

Campbell, C. T., & Peden, C. H. (2005). Oxygen vacancies and catalysis on ceria surfaces. Science, 309(5735), 713-714.

Celardo I, Pedersen JZ, Traversa E, Ghibelli L. Pharmacological potential of cerium oxide nanoparticles. Nanoscale. 2011;3(4):1411-20.

Chen, D., Zhang, G., Li, R., Guan, M., Wang, X., Zou, T., … & Wan, L. J. (2018). Biodegradable, hydrogen peroxide, and glutathione dual responsive nanoparticles for potential programmable paclitaxel release. Journal of the American Chemical Society, 140(24), 7373-7376

Chen, Z. J., Huang, Z., Huang, S., Zhao, J. L., Sun, Y., Xu, Z. L., & Liu, J. (2021). Effect of proteins on the oxidase-like activity of CeO 2 nanozymes for immunoassays. Analyst, 146(3), 864-873

Darroudi, M., Sarani, M., Oskuee, R. K., Zak, A. K., & Amiri, M. S. (2014). Nanoceria: gum mediated synthesis and in vitro viability assay. Ceramics International, 40(2), 2863-2868.

Davies, J., & Wright, G. D. (1997). Bacterial resistance to aminoglycoside antibiotics. Trends in microbiology, 5(6), 234-240.

Dhall, A., & Self, W. (2018). Cerium oxide nanoparticles: a brief review of their synthesis methods and biomedical applications. Antioxidants, 7(8), 97.

Do Dat, T., Cong, C. Q., Nhi, T. L. H., Khang, P. T., Nam, N. T. H., Tinh, N. T., & Hieu, N. H. (2023). Green synthesis of gold nanoparticles using Andrographis paniculata leave extract for lead ion detection, degradation of dyes, and bioactivities. Biochemical Engineering Journal, 200, 109103.

Dowding, J. M., Song, W., Bossy, K., Karakoti, A., Kumar, A., Kim, A., … & Bossy-Wetzel, E. (2014). Cerium oxide nanoparticles protect against Aβ-induced mitochondrial fragmentation and neuronal cell death. Cell Death & Differentiation, 21(10), 1622-1632

Dowding, J. M., Dosani, T., Kumar, A., Seal, S., & Self, W. T. (2012). Cerium oxide nanoparticles scavenge nitric oxide radical (˙ NO). Chemical communications, 48(40), 4896-4898.

Dziubla, T. D., Shuvaev, V. V., Hong, N. K., Hawkins, B. J., Madesh, M., Takano, H., … & Muzykantov, V. R. (2008). Endothelial targeting of semi-permeable polymer nanocarriers for enzyme therapies. Biomaterials, 29(2), 215-227.

Fard, J. K., Jafari, S., & Eghbal, M. A. (2015). A review of molecular mechanisms involved in toxicity of nanoparticles. Advanced pharmaceutical bulletin, 5(4), 447

Griendling, K. K., Touyz, R. M., Zweier, J. L., Dikalov, S., Chilian, W., Chen, Y. R., … & Bhatnagar, A. (2016). Measurement of reactive oxygen species, reactive nitrogen species, and redox-dependent signaling in the cardiovascular system: a scientific statement from the American Heart Association. Circulation research, 119(5), e39-e75.

Heckert, E. G., Karakoti, A. S., Seal, S., & Self, W. T. (2008). The role of cerium redox state in the SOD mimetic activity of nanoceria. Biomaterials, 29(18), 2705-2709

Hossain, S., Urbi, Z., Karuniawati, H., Mohiuddin, R. B., Moh Qrimida, A., Allzrag, A. M. M., … & Capasso, R. (2021). Andrographis paniculata (burm. F.) wall. Ex nees: an updated review of phytochemistry, antimicrobial pharmacology, and clinical safety and efficacy. Life, 11(4), 348.

Ivanov, V. K., Shcherbakov, A. B., & Usatenko, A. V. (2009). Structure-sensitive properties and biomedical applications of nanodispersed cerium dioxide. Russian chemical reviews, 78(9), 855.

Karakoti, A. S., Tsigkou, O., Yue, S., Lee, P. D., Stevens, M. M., Jones, J. R., & Seal, S. (2010). Rare earth oxides as nanoadditives in 3-D nanocomposite scaffolds for bone regeneration. Journal of Materials Chemistry, 20(40), 8912-8919.

Karakoti A, Singh S, Dowding JM, Seal S, Self WT. Redox-active radical scavenging nanomaterials. Chemical Society Reviews. 2010;39(11):4422-32.Kartha, B., Thanikachalam, K., Vijayakumar, N., Alharbi, N. S., Kadaikunnan, S., Khaled, J. M., … & Govindarajan, M. (2022). Synthesis and characterization of Ce-doped TiO2 nanoparticles and their enhanced anticancer activity in Y79 retinoblastoma cancer cells. Green Processing and Synthesis, 11(1), 143-149.

Keyvan Rad, J., Mahdavian, A. R., Khoei, S., & Shirvalilou, S. (2018). Enhanced photogeneration of reactive oxygen species and targeted photothermal therapy of C6 glioma brain cancer cells by folate-conjugated gold–photoactive polymer nanoparticles. ACS applied materials & interfaces, 10(23), 19483-19493

Miri, A., & Sarani, M. (2018). Biosynthesis, characterization and cytotoxic activity of CeO2 nanoparticles. Ceramics International, 44(11), 12642-12647

Montini, T., Melchionna, M., Monai, M., & Fornasiero, P. (2016). Fundamentals and catalytic applications of CeO2-based materials. Chemical reviews, 116(10), 5987-6041.

Mustafa, F., Othman, A., & Andreescu, S. (2021). Cerium oxide-based hypoxanthine biosensor for Fish spoilage monitoring. Sensors and Actuators B: Chemical, 332, 129435.

Nelson, B. C., Johnson, M. E., Walker, M. L., Riley, K. R., & Sims, C. M. (2016). Antioxidant cerium oxide nanoparticles in biology and medicine. Antioxidants, 5(2), 15

Poole, K. M., Nelson, C. E., Joshi, R. V., Martin, J. R., Gupta, M. K., Haws, S. C., … & Duvall, C. L. (2015). ROS-responsive microspheres for on demand antioxidant therapy in a model of diabetic peripheral arterial disease. Biomaterials, 41, 166-175.

Ray, P. D., Huang, B. W., & Tsuji, Y. (2012). Reactive oxygen species (ROS) homeostasis and redox regulation in cellular signaling. Cellular signalling, 24(5), 981-990.

Shuvaev, V. V., Tliba, S., Nakada, M., Albelda, S. M., & Muzykantov, V. R. (2007). Platelet-endothelial cell adhesion molecule-1-directed endothelial targeting of superoxide dismutase alleviates oxidative stress caused by either extracellular or intracellular superoxide. Journal of Pharmacology and Experimental Therapeutics, 323(2), 450-457

Shuvaev, V. V., Han, J., Tliba, S., Arguiri, E., Christofidou-Solomidou, M., Ramirez, S. H., … & Muzykantov, V. R. (2013). Anti-inflammatory effect of targeted delivery of SOD to endothelium: mechanism, synergism with NO donors and protective effects in vitro and in vivo. PLoS One, 8(10), e77002

Singh, K. R., Nayak, V., Sarkar, T., & Singh, R. P. (2020). Cerium oxide nanoparticles: properties, biosynthesis and biomedical application. RSC advances, 10(45), 27194-27214

Singh, S., Kumar, U., Gittess, D., Sakthivel, T. S., Babu, B., & Seal, S. (2021). Cerium oxide nanomaterial with dual antioxidative scavenging potential: Synthesis and characterization. Journal of Biomaterials Applications, 36(5), 834-842.

Sisubalan, N., Ramkumar, V. S., Pugazhendhi, A., Karthikeyan, C., Indira, K., Gopinath, K., … & Basha, M. H. G. (2018). ROS-mediated cytotoxic activity of ZnO and CeO 2 nanoparticles synthesized using the Rubia cordifolia L. leaf extract on MG-63 human osteosarcoma cell lines. Environmental Science and Pollution Research, 25, 10482-10492.

Thammawithan, S., Talodthaisong, C., Srichaiyapol, O., Patramanon, R., Hutchison, J. A., & Kulchat, S. (2022). Andrographolide stabilized-silver nanoparticles overcome ceftazidime-resistant Burkholderia pseudomallei: study of antimicrobial activity and mode of action. Scientific Reports, 12(1), 10701.

Tian, Z., Liu, H., Guo, Z., Gou, W., Liang, Z., Qu, Y., … & Liu, L. (2020). A pH-responsive polymer-ceO2 hybrid to catalytically generate oxidative stress for tumor therapy. Small, 16(47), 2004654.

Xia, T., Kovochich, M., Liong, M., Madler, L., Gilbert, B., Shi, H., … & Nel, A. E. (2008). Comparison of the mechanism of toxicity of zinc oxide and cerium oxide nanoparticles based on dissolution and oxidative stress properties. ACS nano, 2(10), 2121-2134.

Xu, C., & Qu, X. (2014). Cerium oxide nanoparticle: a remarkably versatile rare earth nanomaterial for biological applications. NPG Asia materials, 6(3), e90-e90.

Xu, C., Lin, Y., Wang, J., Wu, L., Wei, W., Ren, J., & Qu, X. (2013). Nanoceria-triggered synergetic drug release based on CeO2-capped mesoporous silica host–guest interactions and switchable enzymatic activity and cellular effects of CeO2. Advanced healthcare materials, 2(12), 1591-1599.

Yadav, S., Sharma, S., Ahmad, F., & Rathaur, S. (2020). Antifilarial efficacy of green silver nanoparticles synthesized using Andrographis paniculata. Journal of Drug Delivery Science and Technology, 56, 101557.

Yeh, H. P., Del Valle, A. C., Syu, M. C., Qian, Y., Chang, Y. C., & Huang, Y. F. (2018). A new photosensitized oxidation-responsive nanoplatform for controlled drug release and photodynamic cancer therapy. ACS applied materials & interfaces, 10(25), 21160-21172.

Yokel, R. A., Hussain, S., Garantziotis, S., Demokritou, P., Castranova, V., & Cassee, F. R. (2014). The yin: an adverse health perspective of nanoceria: uptake, distribution, accumulation, and mechanisms of its toxicity. Environmental Science: Nano, 1(5), 406-428.

Zhao, Y., Li, H., Lopez, A., Su, H., & Liu, J. (2020). Promotion and Inhibition of the Oxidase-Mimicking Activity of Nanoceria by Phosphate, Polyphosphate, and DNA. ChemBioChem, 21(15), 2178-2186.